

Jaret, S. J., Tailby, N. D., Hammond, K., Rasbury, E. T., Wooton, K., Ebel, D. S., Plank, T., Dipadova, E., Yuan, V., Smith, R., Jaffe, N., Smith, L. M., and Spaeth, L. 2023, The Manhattan project: Isotope geochemistry and detrital zircon 18 geochronology of schists in New York City, USA: GSA Bulletin, <https://doi.org/10.1130/B37024.1>.

## Supplemental Material

**Supplemental Text S1:** The supplemental text includes methods for sample preparation, chemistry, and instrument parameters for zircon and Nd analysis.

**Table S1.** Sample locations, eNd value, and detrital zircon population ages for Schists of New York City.

**Table S2.** Intrasample comparison statistics for schists of New York City and southern New England

**Figure S1.** Plane polarized light and cross polarized light optical photomicrographs of PB18-9

**Figure S2:** Plane polarized light and cross polarized light optical photomicrographs of TP-05.

**Figure S3:** Plane polarized light and cross polarized light optical photomicrographs of TP-06.

**Figure S4.** Plane polarized light and cross polarized light optical photomicrographs of E79.

**Figure S5.** Plane polarized light and cross polarized light optical photomicrographs of RNHE.

**Figure S6.** Plane polarized light and cross polarized light optical photomicrographs of RNHW.

**Figure S7.** Plane polarized light and cross polarized light optical photomicrographs of AMNH-GS-11.

**Figure S8.** Plane polarized light and cross polarized light optical photomicrographs of GWB

**Figure S9.** Select CL images of zircons from AMNH-GS-11

**Figure S10:** Probability Cumulative Plot and Cumulative Distribution Frequency plot for zircons ages.

## Supplemental Text S1: Methods

### **Detrital Zircon**

#### ***Sample Preparation***

Samples were crushed using a Bico disc mill after hand crushing, before being sieved to between 63 and 250 microns and swept with a hand magnet to remove magnetic grains and any metal contamination from the grinder. Minerals were separated using a Frantz isodynamic separator, under successively higher current: 0.2A, 0.6 A, and 1.0 A. The non-magnetic fraction was processed for density separation using Sodium Polytungstate ( $\rho=2.9 \text{ cm/cm}^3$ ). Zircons were then hand-picked from the dense fraction then and mounted in epoxy and polished to expose the center of the grains ensuring that laser spots would not sampling through multiple growth zones as the laser ablated through the grain. Limited cathodoluminescence (CL) images of some samples were acquired prior to analysis (see Supplement). Most samples were CL inactive. Based on the few CL images available, spot locations were selected to sample the center of the polished grains, and U, Pb, and Ti concentrations were tracked in real-time during analysis providing confidence that only single zones were sampled.

#### ***Zircon Mass Spectrometry***

Zircons for samples AMNH Gilder, RNHW, RNHE, E79th St, and PB18-9 were measured using an Agilent 7500-ce quadrupole mass spectrometer equipped with a New Wave 213 nm solid state laser at the Facility for Isotope Research and Student Training (FIRST) laboratory at Stony Brook University. The Agilent was tuned specifically for high mass with an Ar plasma and He carrier gas. The laser was run at 10 Hz and fluence of  $0.32 \text{ J/cm}^2$ . All spots were 30 microns circles. Counting time on mass 49, 204, 206, 207, 208, 235, and 238 were 0.1 sec. Each analysis was a 30 sec dwell time, and time was allowed for the signal to return to baseline between spots. Data reduction was conducted in Iolite using the U-Pb geochronology Data Reduction Scheme

(Paton et al., 2011). The primary natural reference material was the Mud Tank (age= 730 Ma, Black and Gulson, 1978) with Plesovice zircon (age = 338 Ma, Slama et al., 2008) acting as a secondary standard. By combined observations from primary and secondary standards, minimal drift was observed among the mass sweep and reported ratios from reference materials are in agreement with published values. The unknown zircons were screened for concordance using the following equation: % discordance =  $(1 - ((^{206}\text{Pb}/^{238}\text{U}_{\text{date}} / ^{207}\text{Pb}/^{235}\text{U}_{\text{date}})) * 100$ . Grains with % discordance greater than 15% were excluded from the plots. Ages reported are  $^{206}\text{Pb}/^{238}\text{U}$  ages for grains younger than 1500 Ma and  $^{207}\text{Pb}/^{206}\text{Pb}$  ages for grains older than 1500 Ma (Spencer et al. 2016).

FL-3 and NYC14-TAP-22 were measured separately at Washington State University. Heavy mineral concentrates of the <350  $\mu\text{m}$  fraction from all samples were separated using traditional techniques at ZirChron LLC. Zircons from the non-magnetic fraction were handpicked under the microscope and mounted in a 1-inch diameter epoxy puck and slightly ground and polished to expose the surface and keep as much material as possible for laser ablation analyses. After CL imaging, the LA-ICP-MS U-Pb analyses were conducted using a New Wave Nd:YAG UV 213-nm laser coupled to a ThermoFinnigan Element 2 single collector, double-focusing, magnetic sector ICP-MS. Operating procedures and parameters are similar to those of Chang et al. (2006). Laser spot size and repetition rate were 30 microns and 10 Hz, respectively. He and Ar carrier gases delivered the sample aerosol to the plasma. Each analysis consists of a short blank analysis followed by 250 passes through masses 202, 204, 206, 207, 208, 232, 235, and 238, taking approximately 30 seconds. Time-independent fractionation was corrected by normalizing U/Pb and Pb/Pb ratios of the unknowns to the reference zircon standards (Chang et al., 2006). U and Th concentration were monitored by comparing to NIST 610 trace element glass. Two reference

zircon standards were used: Plesovice, with an age of 338 Ma (Slama et al., 2010) and FC-1, with an age of 1099 Ma (Paces and Miller, 1993). Uranium-lead ages were calculated using Isoplot (Ludwig, 2003). U-Pb zircon crystallization ages errors are reported using quadratic sum of the analytical error plus the total systematic error for the set of analyses.

### **Nd Chemistry**

Powdered samples (0.08 g) were dissolved in 4 ml HNO<sub>3</sub> + 200 µl HF followed by a 1:1 M (by volume) of HNO<sub>3</sub> and HCl. The acid dissolution process was performed in capped Teflon beakers on a hot-plate where temperature was held at constant 180 °C. After dissolution, all Nd separation was conducted following a standard 2-step column chemistry process: REEs were separated using Eichrom TRU Spec resin loaded in 1.4N HNO<sub>3</sub> and eluted in 1N HCl. The Nd was then further separated from the other REEs using Eichrom LnSpec resin loaded and eluted in 0.22N HNO<sub>3</sub>.

### **Nd Mass Spectrometry**

The Nd cut was diluted to 50 ppb and analyzed on a Nu II multi-collector Inductively coupled plasma mass spectrometer (MC-ICP-MS) in the FIRST lab at Stony Brook University. Samples were bracketed by an internal 50 ppb Nd solution and standardized with 50 ppb the standard jNdi solution (<sup>143</sup>Nd/<sup>144</sup>Nd value of 0.512107 ± 7 per Tanaka et al., 2000).

### **References:**

- Black, L.P. and Gulson B.L., 1978, The age of the Mud Tank Carbonatite, Strangways Range, Northern Territory: *Journal of Australian Geology and Geophysics*, v. 3, p. 227–232.
- Paces, J.B., and Miller, J.D., 1993, U-Pb ages of the Duluth Complex and related mafic intrusions, northeastern Minnesota: geochronologic insights into physical, paleomagnetic and tectonomagmatic processes associated with the 1.1 Ga mid-continent rift system: *Journal of Geophysical Research*, v. 98, no. B8, p. 13997-14013.

Paton, C., Hellstrom, J. C., Paul, B., Woodhead, J. D., and Hergt, J. M., 2011, Iolite: Freeware for the visualisation and processing of mass spectrometric data *J. Anal. At. Spectrom.*, 2011, **26**, 2508 —2518.

Slama, J., Kosler, J., Condon, D.J., Crowley, J.L., Gerdes, A., Hanchar, J.M., Whitehouse, M. J., 2008,. Plesovice zircon : A new natural reference material for U-Pb and Hf isotopic microanalysis. *Chemical Geology*, 2491–35. <https://doi.org/10.1016/j.chemgeo.2007.11.005>

Tanaka, T., Togashi, S., Kamioka, H., Amakawa, H., Kagami, H., Hamamoto, T., Yuhara, M., Orihashi, Y., Yoneda, S., Shimizu, H. and Kunimaru, T., 2000. JNdi-1: a neodymium isotopic reference in consistency with LaJolla neodymium. *Chemical Geology*, 168(3-4), pp.279-281.

## Figure Captions

S1: Plane polarized light and cross polarized light optical photomicrographs of PB18-9

S2: Plane polarized light and cross polarized light optical photomicrographs of TP-05.

S3: Plane polarized light and cross polarized light optical photomicrographs of TP-06.

S4: Plane polarized light and cross polarized light optical photomicrographs of E79.

S5: Plane polarized light and cross polarized light optical photomicrographs of RNHE.

S6: Plane polarized light and cross polarized light optical photomicrographs of RNHW.

S7: Plane polarized light and cross polarized light optical photomicrographs of AMNH-GS-11.

S8: Plane polarized light and cross polarized light optical photomicrographs of GWB

S9: Select CL images of zircons from AMNH-GS-11

S10: Probability Cumulative Plot and Cumulative Distribution Frequency plot for zircons ages.

Dataset 1 is RNHW. Dataset 2 is RNHE. Dataset 3 is TAP-NYC-22. Dataset 4 is E79. Dataset 5 is PB19-5. Dataset 6 is FL3. Dataset 7 is Moretown (Macdonald et al., 2014). Dataset 8 is Nashoba (Waldron et al., 2022). Dataset 9 is Price Neck Fm. (Kuiper et al. 2022). Dataset 10 is Rowe

(Macdonald et al., 2014). Dataset 11 is Hawley (Macdonald et al., 2014). Dataset 12 is Taconic Allochthon (Waldron et al., 2022)



Figure S1, PB18-9

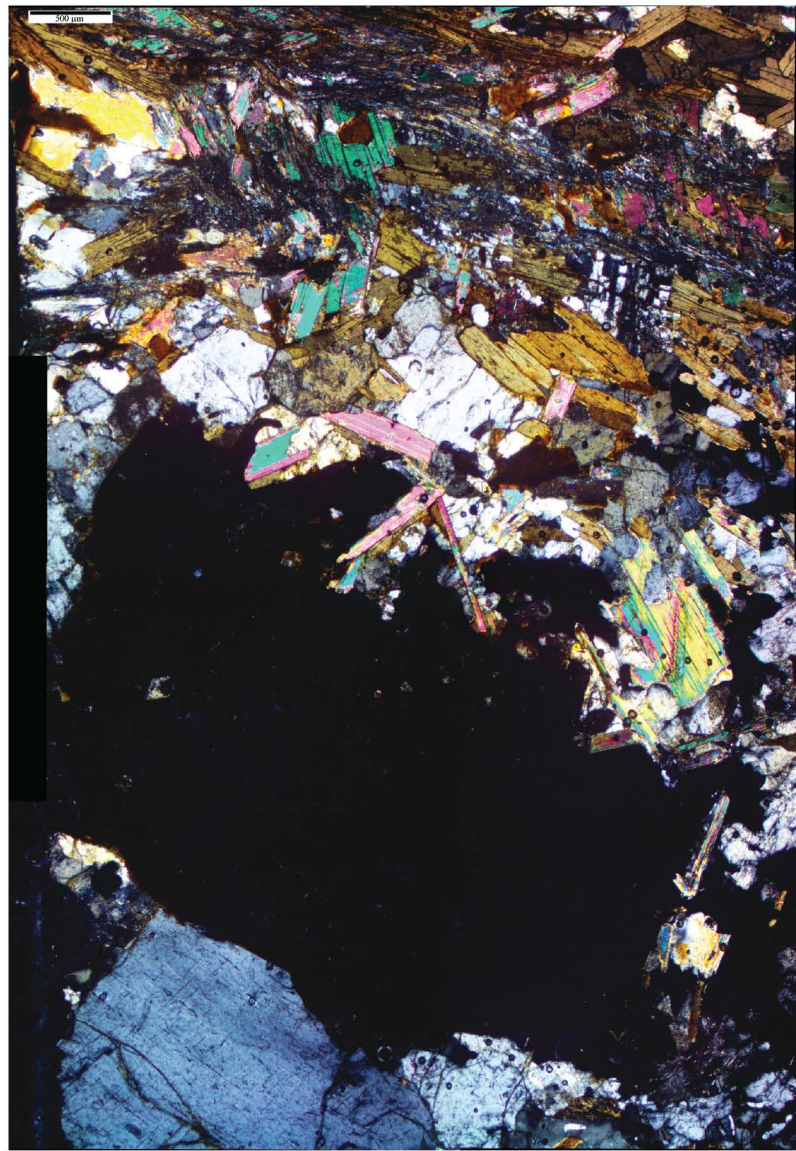
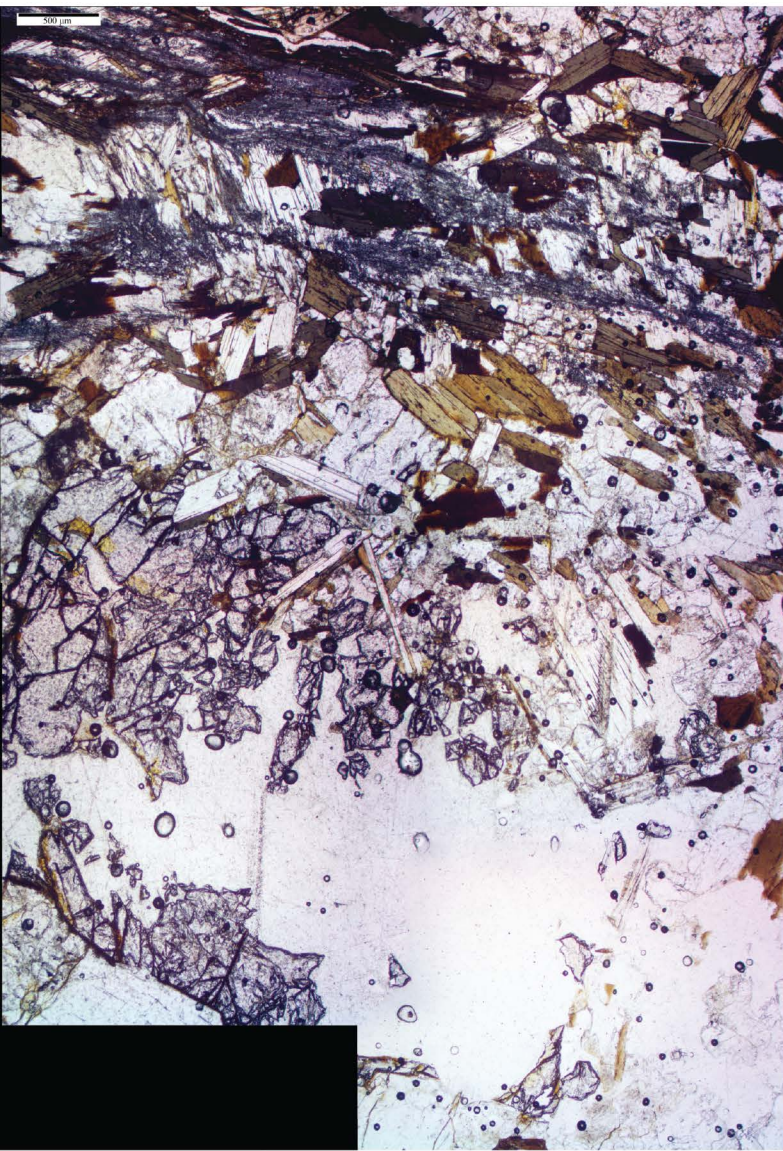




Figure S2 TP-05

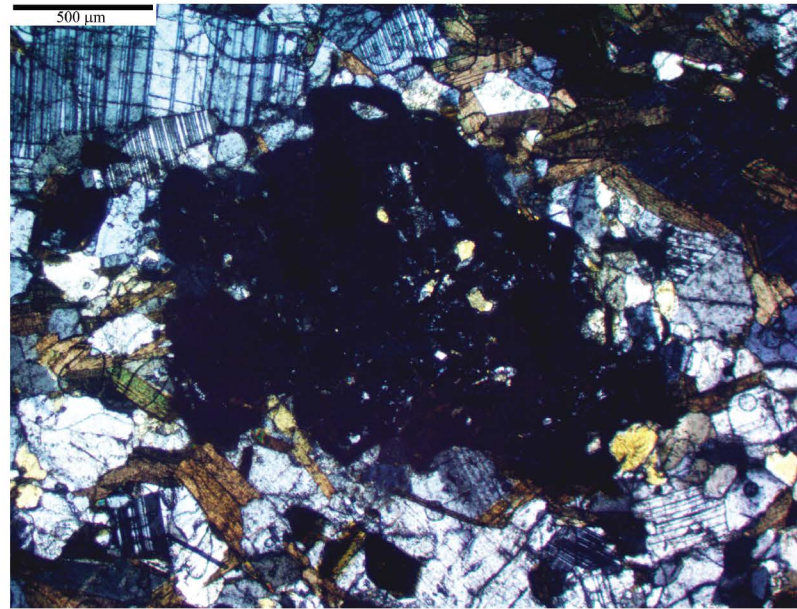
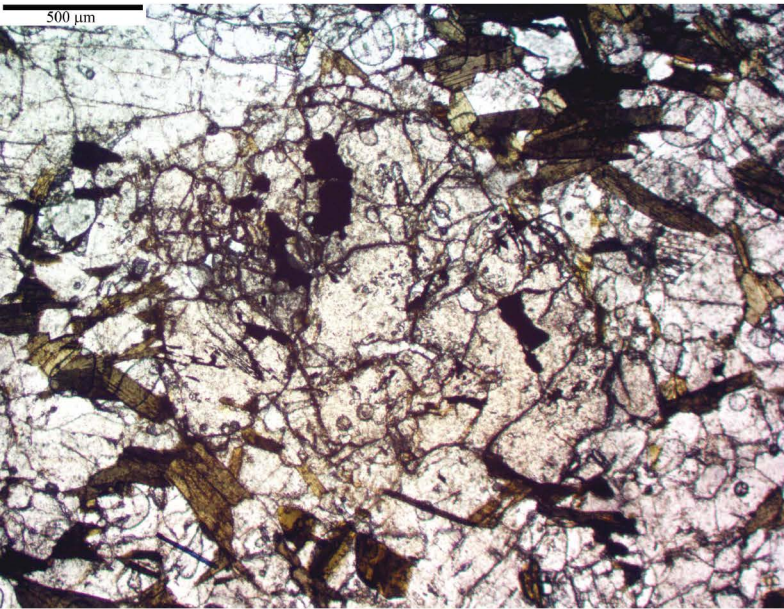




Figure S3, TP-06

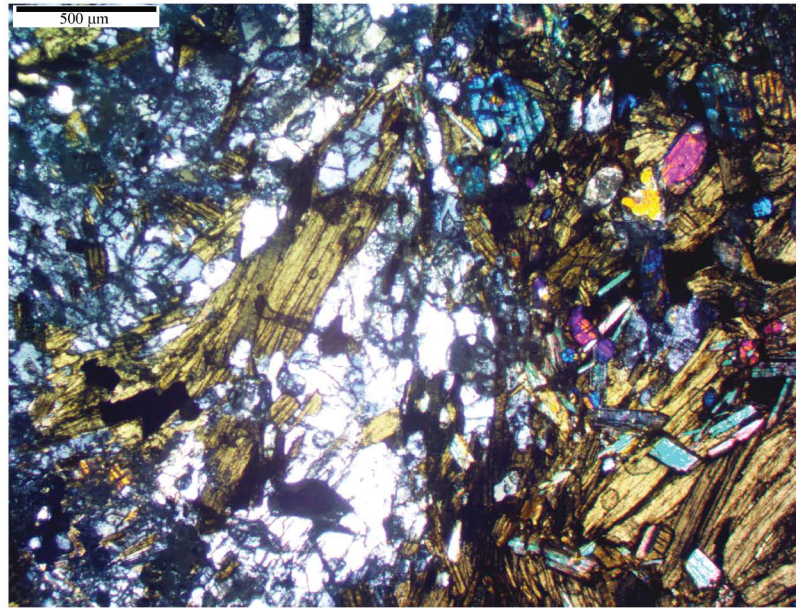
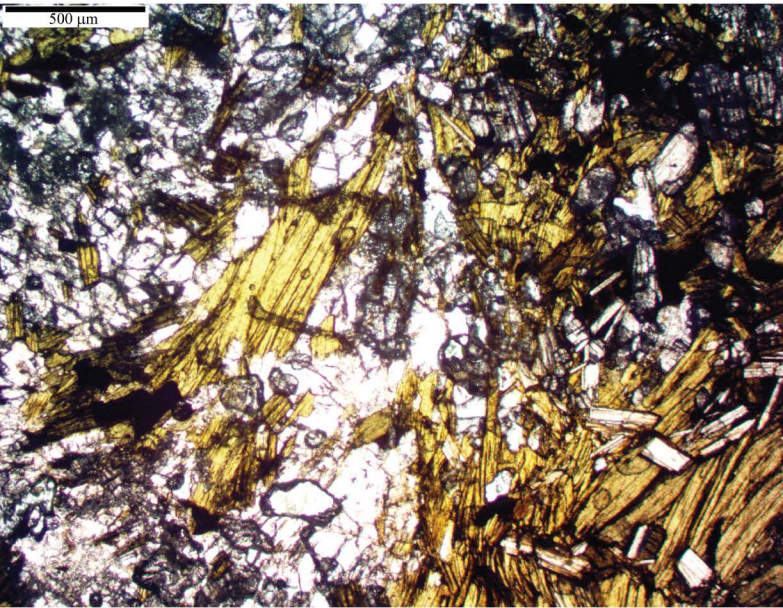


Figure S4: E79th

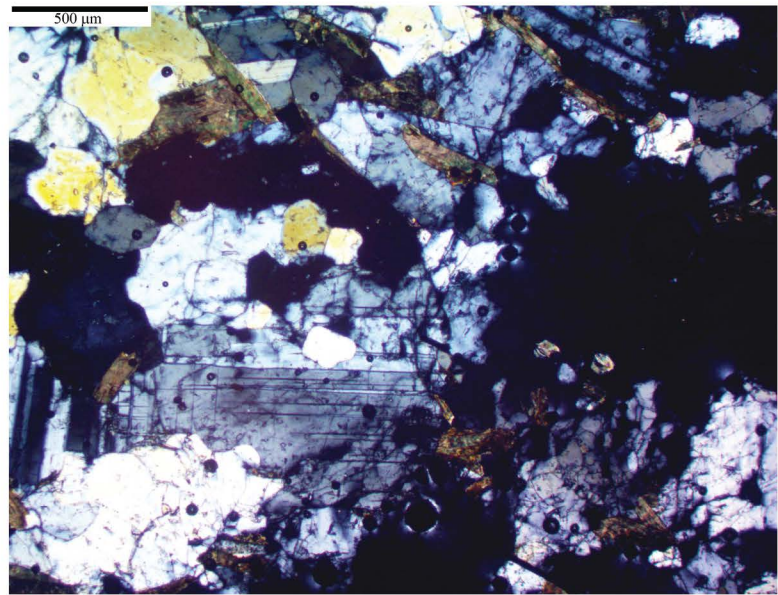
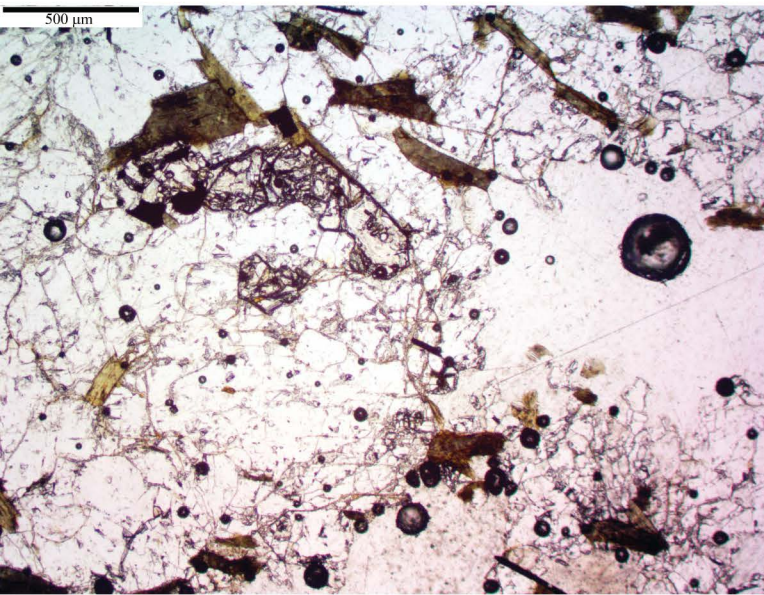




Figure S5 RNHE

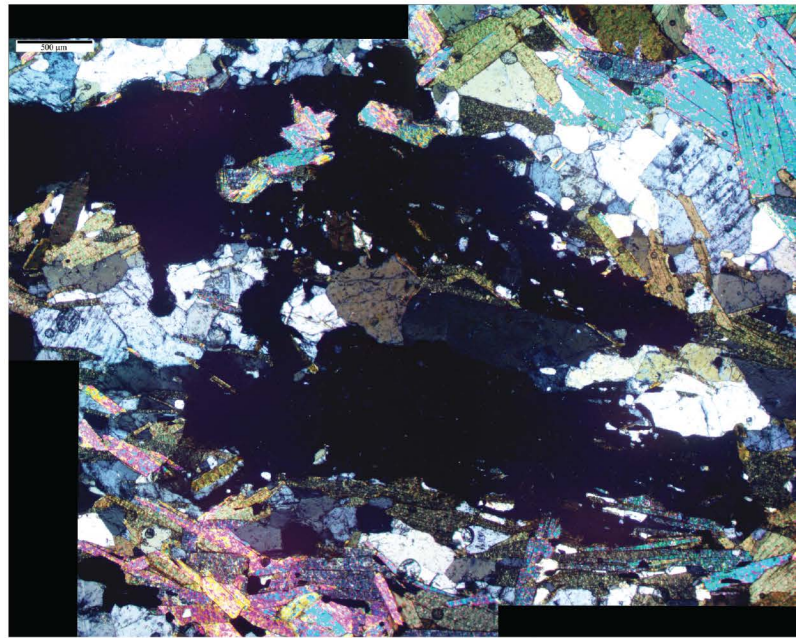
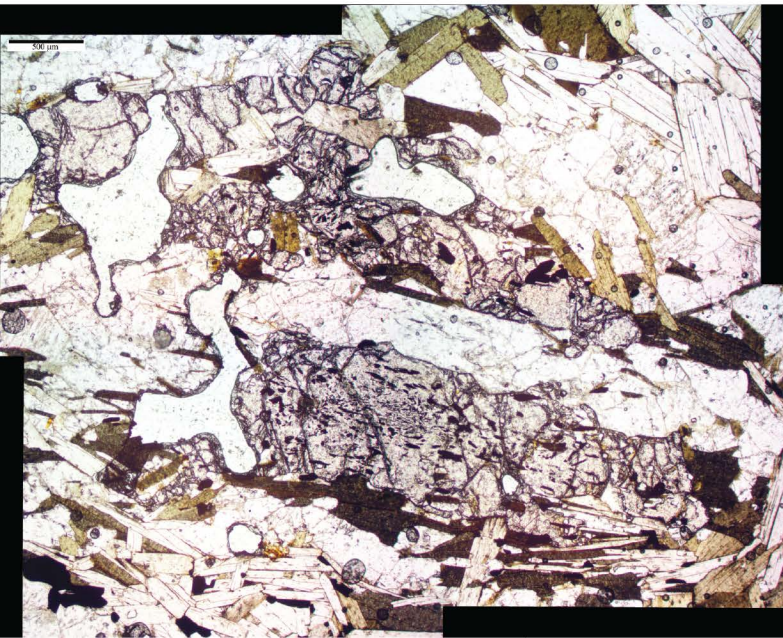


Figure S6 RNHW

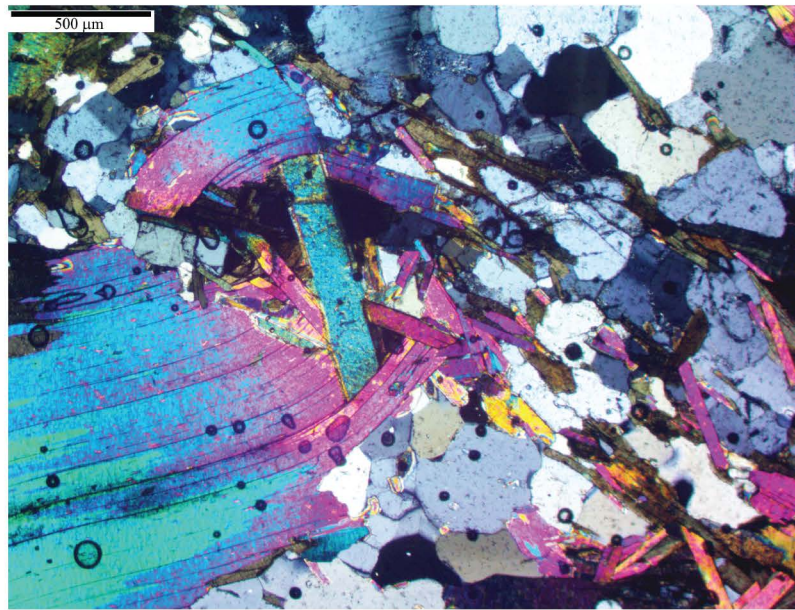
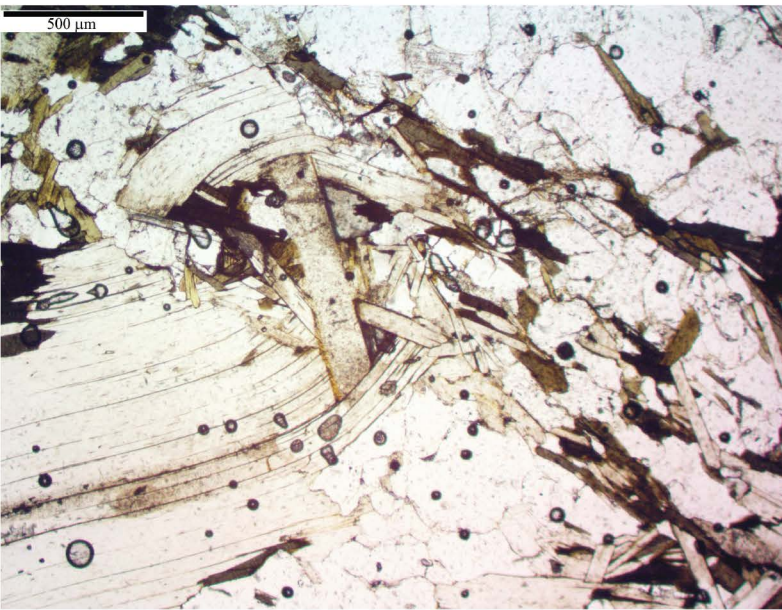




Figure S7 AMNH-GS-11

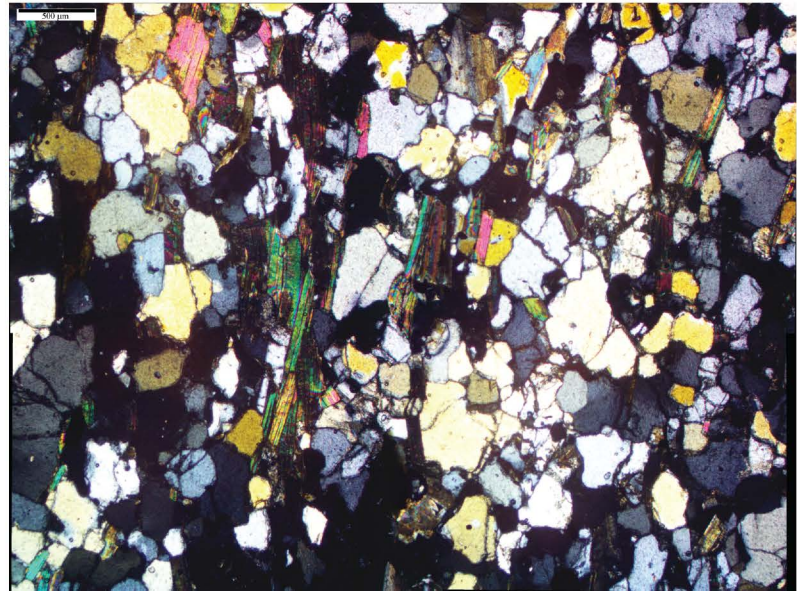
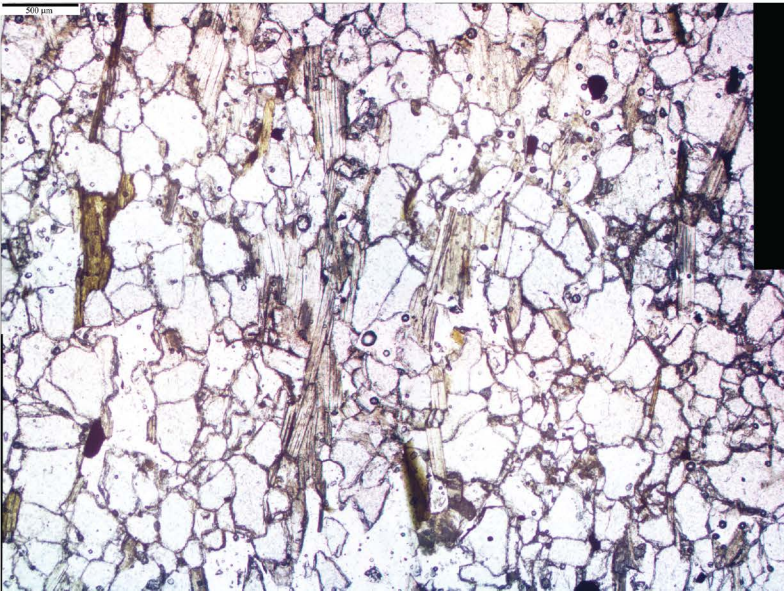
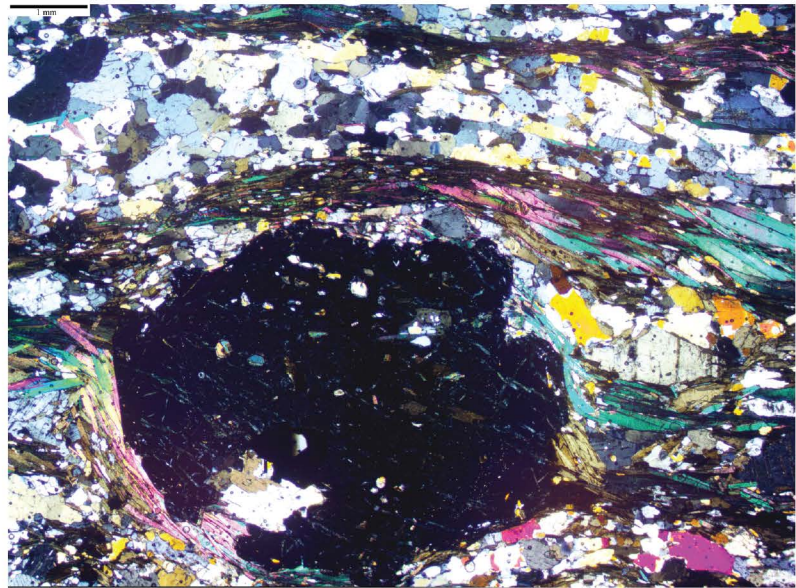
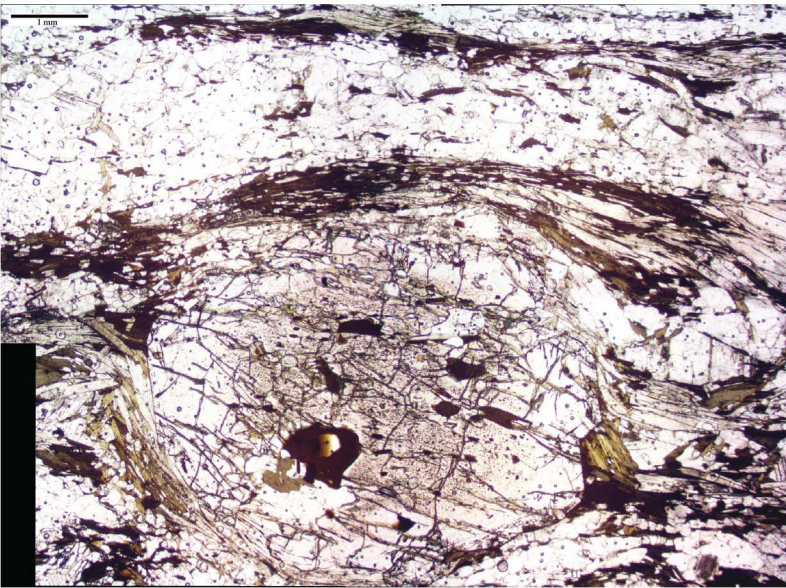




Figure S8 GWB



# AMNH-GS-11

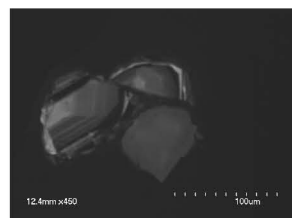
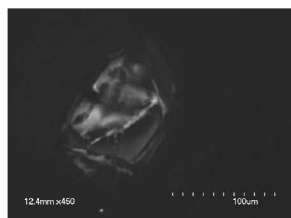
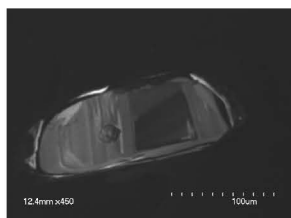
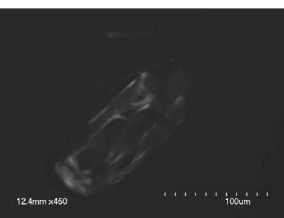
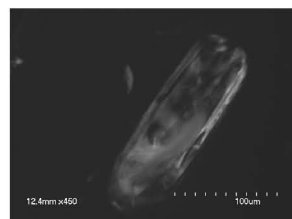
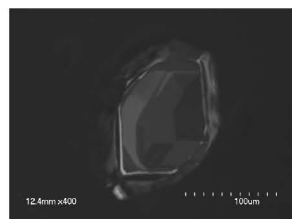
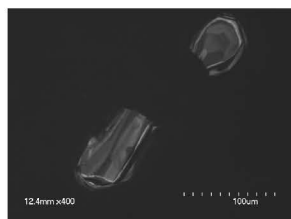
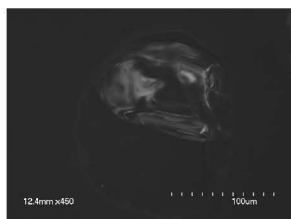
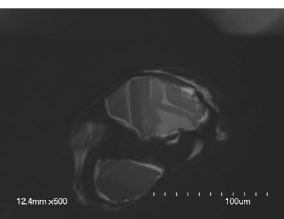
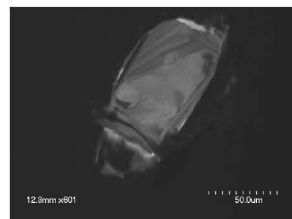
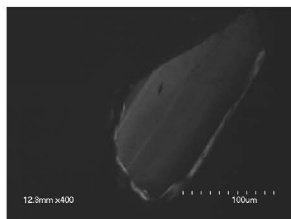
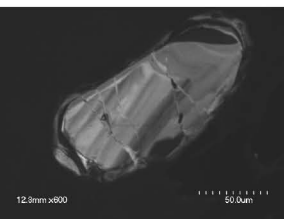
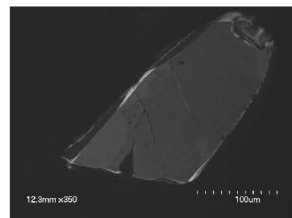
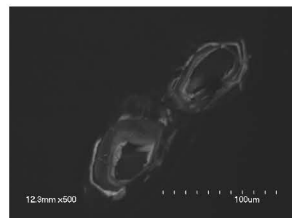
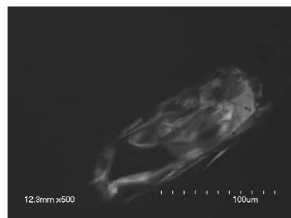
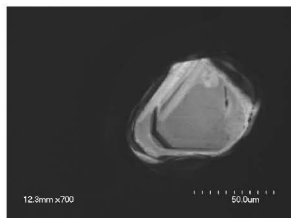
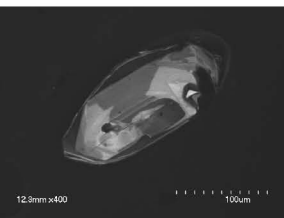


Figure S10:

